THE 0.4 ARC-SEC TANDEM-X INTERMEDIATE DEM WITH RESPECT TO THE SRTM AND THE ASTER GLOBAL DEMS: EXTENDED

Dimitra Vassilaki and Thanasis Stamos

National Technical University of Athens, Athens, Greece;
dimitra.vassilaki@gmail.com, stamthan@central.ntua.gr

ABSTRACT

This paper studies a preliminary version of the forthcoming TanDEM-X DEM, a new global 3D model of the Earth's surface. The TanDEM-X IDEM is studied with respect to two well-known and much used existing global DEMs, the ASTER and the SRTM, using local DEM and DSM data over a few test sites in the area of the Aegean islands. Computed results show that TanDEM-X IDEM is dramatically enhanced with respect to existing global DEMs and that it is accompanied by metadata that offer a more enhanced use of the final DEM. For further research bathymetric data can be taken into account. The study of TanDEM-X IDEM with respect to DEMs produced by satellite optical images is also intriguing.

INTRODUCTION

A new global DEM is about to appear: the TanDEM-X DEM [1]. TanDEM-X DEM is currently collected by two twin high resolution X-band satellite SAR sensors, TerraSAR-X and TanDEM-X. TerraSAR-X and TanDEM-X were launched in 2007 and 2010 respectively with 5 years life-time and they are still in operation. The two identical satellite SAR sensors are flying in close formation and operate practically like a single-pass interferometer that simultaneously collects pairs of high resolution SAR data of the Earth's surface [2, 3]. The mission is classified to the state-of-the-art mapping technologies for many reasons (very high resolution imaging mode, enhanced radiometric quality, high geolocation accuracy etc) but the main innovation is related to its main objective: the collection and the computation of a new accurate, high resolution, homogeneous global 3D model of the Earth's surface. In order to create a first impression of the forthcoming TanDEM-X DEM a preliminary version, namely TanDEM-X Intermediate DEM (IDEM), became recently available to the scientific community. According to the specifications [4], the TanDEM-X IDEM was computed using data collected only during the first global coverage and is expected to be of lower quality (e.g. existence of gaps, increased height error) than the final DEM, especially for areas of the world which suffer most from layover and shadow effects (e.g. mountainous regions). It is available with pixel spacing 0.4, 1 and 3 arc-sec with absolute planar and vertical accuracy better than 10 m and undefined relative vertical accuracy (the nominal relative vertical accuracy of the final DEM will be better than 2 m for flat areas and 4 m for areas with slope greater to 20%). The TanDEM-X IDEM is available for specific areas of the world, one of which is the Aegean archipelago used in this paper. So far, [5] studied TanDEM-X IDEM with respect to existing global DEMs and [6] used it to derive catchment properties.

This paper follows [5] which studied the TanDEM-X IDEM with respect to the SRTM and the ASTER global DEMs through visual inspection and computation of the error of all three DEMs with respect to local elevation data (national archive DEM and national network of triangulation pillars), over a few test sites on Aegean islands (Figure 1). Aegean islands are a special case of the Earth's surface as they exhibit: lack of forested areas, absence of tall buildings, large number of scattered islands of various sizes with irregular and ragged (not flat) terrain. It is considered to be a difficult area for satellite SAR mapping as it is affected by shadow and layover effects (Figure 1) [1]. The present paper extends the study using more, and more accurate elevation data, over more test sites on Aegean islands, and exploiting the metadata provided with TanDEM-X IDEM:

1. National recent DEM and DSM are used as reference data for the computation of the 3D

vector displacement of the global DEMs which minimises the RMSE of the elevations combining exhaustive search and divide-and-conquer algorithms [7]. The process is applied to all three global DEMs in order to gain a perspective of the results.

2. The Height Error Map (HEM) metadata which accompanies the TanDEM-X data is taken into account for the computation of a more realistic displacement between TanDEM-X DEM and local/national elevation data.

The present study verifies that there is strong evidence that the forthcoming TanDEM-X DEM is going to be dramatically enhanced with respect to the other two global DEMs.

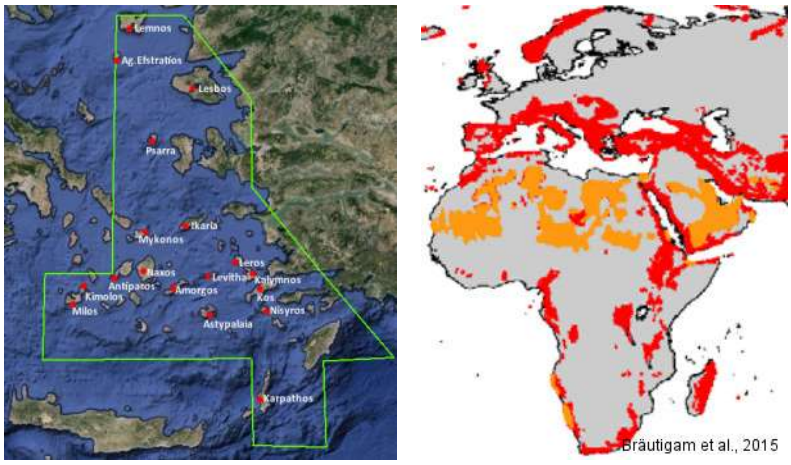

Figure 1: The study site (left). Regions affected by shadow and layover effects (in red) have been identified from terrain slope calculations [1].

METHODOLOGY

Global DEMs such as TanDEM-X IDEM are optimised for the whole surface of the Earth. Local DEMs are naturally optimised for the specific area of the Earth they model. Consequently it is possible that there may be a systematic displacement, or bias, between the global and local DEM, both horizontal and vertical. In order to find the horizontal bias a criterion of the closeness between the DEMs must be defined. The obvious choice is the Root Mean Squared Error (RMSE) between the DEMs:

$$RMSE = \sqrt{\frac{1}{n}\sum_{i=1}^{n}\left[z_i^L - f^G(x_i^L, y_i^L)\right]^2} \quad (1)$$

where $f^G(x,y)$ is the function which returns the elevation of the global DEM at a point with coordinates x, y and x_i^L, y_i^L, z_i^L are the coordinates of the nodes/grid points of the local DEM, assuming that the local DEM has denser nodes/grid points than the global DEM. The horizontal bias (DX, DY) between the global and local DEM is found with exhaustive search. The global DEM is displaced by all (within reason) possible values of DX, DY, and for each pair of (DX, DY) the RMSE is computed:

$$RMSE = \sqrt{\frac{1}{n}\sum_{i=1}^{n}\left[z_i^L - f^G(x_i^L - DX, y_i^L - DY)\right]^2} \quad (2)$$

The pair (DX^b, DY^b) which gives the least RMSE is the bias between the DEMs. Once (DX^b, DY^b) is computed, and assuming a vertical bias DZ between the DEMs the following equation must hold:

$$z_i^L = f^G(x_i^L - DX^b, y_i^L - DY^b) + DZ \quad (3)$$

The best value of the vertical bias DZ^b is found by applying linear Least Squares Adjustment (LSA) to equation (3). The computational cost of the methodology as described is high but it can be reduced with a combination of the exhaustive search and the divide-and-conquer algorithms. More details can be found in [5, 7].

The TanDEM-X IDEM differs than other global DEMs because it is accompanied by a rich set of metadata, one of which is the Height Error Map (HEM). HEM gives the expected error in meters of each height of the DEM. This is very useful when the TanDEM-X IDEM is used in practical applications as it gives an estimate of the height error in the area it is used. Of course if a more accurate local DEM is available, HEM is of little use as the difference between the two DEMs can be reliably found by equation (1). Incorporation of the HEM into equation (1) would in fact lead to a less objective RMSE, as HEM is part of TanDEM-X IDEM and the RMSE must be computed with independent control information.

However HEM is very useful in the computation of more realistic values of the horizontal bias (DX, DY). In equation (2) both the TanDEM-X IDEM and the local DEM are used as control information for the computation of (DX, DY), and thus exploiting the full information of TanDEM-X IDEM (DEM and HEM) leads to better results. Assume that a bias (DX_1, DY_1) led to the same RMSE as another bias (DX_2, DY_2), with the difference that (DX_1, DY_1) were such that all coordinates $x_i^L - DX_1, y_i^L - DY_1$ corresponded to heights with large errors as indicated by HEM, while (DX_2, DY_2) were such that all coordinates $x_i^L - DX_2, y_i^L - DY_2$ corresponded to heights with small errors as indicated by HEM. The immediate conclusion would be that the first RMSE (due to (DX_1, DY_1)) is not as reliable as the second RMSE (due to (DX_2, DY_2)), or that (DX_2, DY_2) is preferable. Thus the criterion of closeness between TanDEM-X IDEM and a local DEM (equation 2) should take into account that height error provided by HEM as a means of the reliability of each point. In other words the weight of each point should be the inverse of its corresponded height error:

$$RMSE = \sqrt{\frac{1}{W}\sum_{i=1}^{n} w_i \left[z_i^L - f^G(x_i^L - DX, y_i^L - DY) \right]^2} \qquad (4)$$

where $w_i = \frac{1}{\left[HEM(x_i^L - DX, y_i^L - DY) \right]^2}$, $W = \sum_{i=1}^{n} w_i$

It should be noted that the RMSE of equation (4) is used only as a closeness criterion for the computation of the bias (DX, DY). Once the best values of the bias (DX^b, DY^b) are computed, the difference of the two DEMs is computed by equation (2) which is independent to HEM. It should also be noted that generally when (DX^b, DY^b) is computed using weights, the RMSE computed by equation (2) is larger than the RMSE without using weights. However the bias (DX^b, DY^b) computed using weights is more realistic as it relies mostly to heights with less error.

APPLICATION

The methodology is applied to TanDEM-X IDEM with respect to more accurate local DEMs. In order to gain a perspective of the results the methodology is also applied to the ASTER and SRTM global DEMs. The data sets used in this study are the ASTER, the SRTM and the TanDEM-X IDEM and they are described in [5]. A local recent DEM (named recent DEM hereafter) and a local recent DSM (named DSM hereafter) are used as reference information. Both the recent DEM and DSM were produced photogrammetrically in 2008 using optical aerial images. The pixel size of the recent DEM is 5 m, while the absolute and relative vertical accuracy is 4 m and 2 m respectively. The pixel size of the DSM is 0.80 m while the absolute and relative vertical accuracy is 1.2 and 0.60 m respectively. The three global DEMs (ASTER, SRTM and TanDEM-X IDEM) are studied using as reference the recent DEM and DSM over three study sites: 1) Psarrou, Mykonos island, 2) Chora, Chios island and 3) Vathi, Samos island. The selection of the study sites is random, as it

was based solely on the availability of data. The Psarrou study site in Mykonos coincides with a study site of [5] and is described in [5]. The coverage of the recent DEM and DSM are the same in Psarou, Mykonos, while in the other two study sites the coverage of the recent DEM is larger than that of the DSM. The Chora study site is located in the east of the Chios island and it is suburban area with low buildings and various cultivated fields. The Vathi study site is located in the north of the Samos island and it is also a similar suburban area.

Table 1: RMSE of the 3 global DEMs over the 3 sites with respect to the recent DEM and DSM. (DX,DY,DZ)=(0,0,0).

Ref.	$RMSE_{original}$	ASTER	SRTM	TanIDEM-X
Archived DEM	Psarrou, Mykonos	9.0	8.4	2.6
Recent DEM	Psarrou, Mykonos	9.1	6.8	2.6
	Chora, Chios	9.1	6.3	3.1
	Vathi, Samos	8.4	13.1	2.2
DSM	Psarrou, Mykonos	9.5	7.3	2.7
	Chora, Chios	8.1	6.0	3.0
	Vathi, Samos	8.8	12.0	3.4

Initially the RMSE (equation 1) was computed of each global DEM with respect to the recent DEM and the DSM (Table 1). For the Psarrou site the RMSE was also computed with respect to an archived DEM digitised from an old, medium scale, archived paper map [5]. The height difference maps and histograms between global and local DEMs are shown in Figures 2, 3. It is clear that TanDEM-X IDEM is more than 2 times better than the other 2 global DEMs. Furthermore, TanDEM-X IDEM's histogram is much sharper, meaning that the magnitude of the height differences is limited near the RMSE.

Subsequently, the horizontal bias (DX, DY) and the vertical bias (DZ) between the global DEMs and the recent DEM and DSM (equations 2, 3) were computed. Table 2 shows (DX, DY) and DZ as well the corresponding RMSEs. Figure 4 shows the RMSE with no bias, RMSE with bias (DX,DY), and RMSE with bias (DX,DY,DZ) for all cases. The bias (DX, DY) of TanDEM-X IDEM is small and almost always smaller than both ASTER and SRTM, while the bias DZ is practically non-existent. The RMSE with (DX, DY) and (DX, DY,DZ) is again smaller than both ASTER and SRTM (about half or smaller). This is shown clearly in Figure 4.

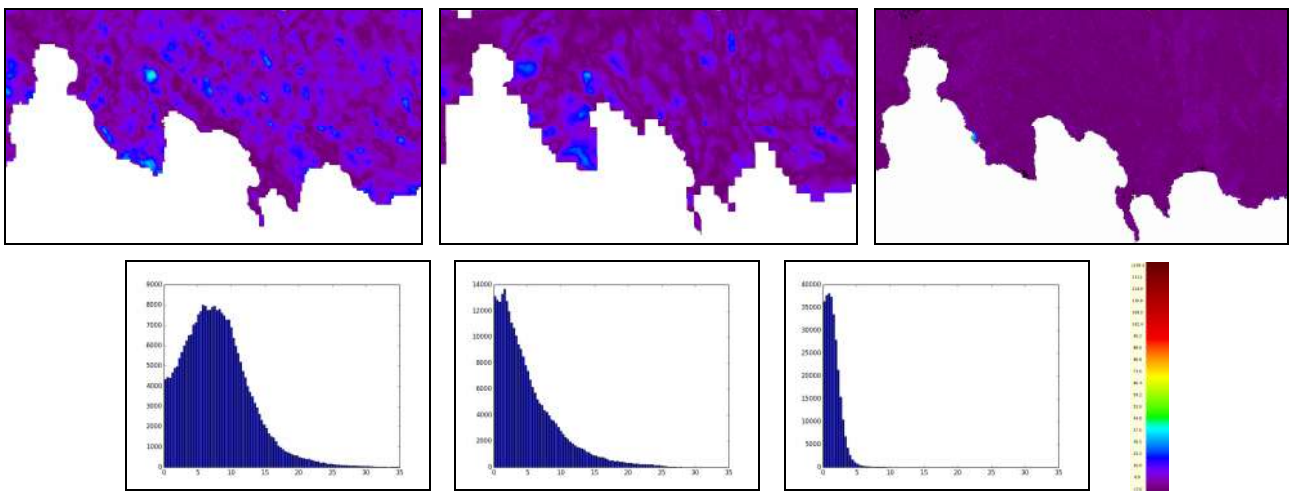

Figure 2: The elevation differences between global DEMs and the recent DEM in Psarrou, Mykonos. ASTER: left, SRTM: middle, TanDEM-X IDEM: right. (DX,DY,DZ)=(0,0,0).

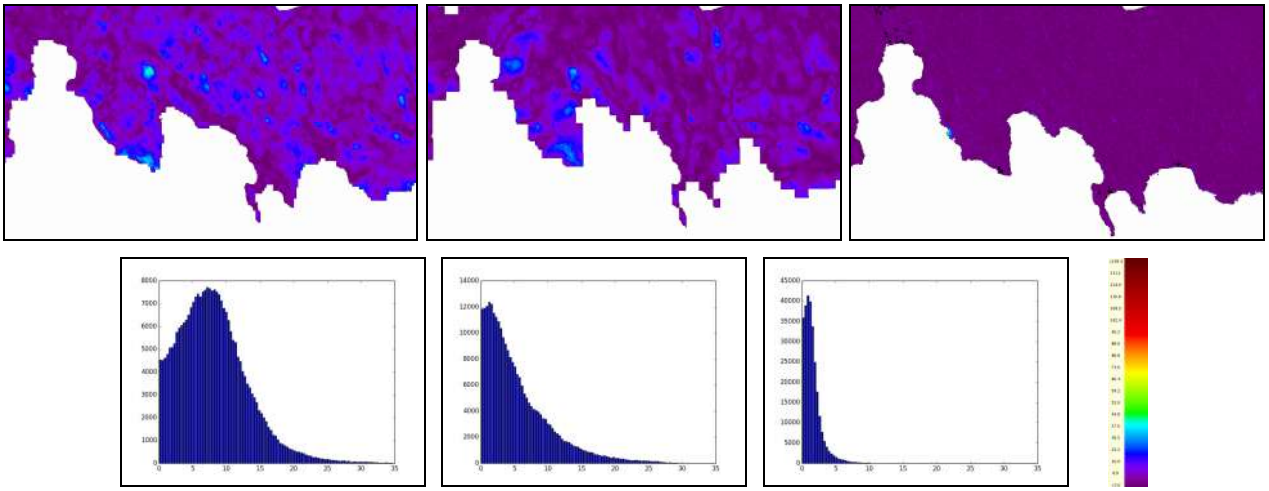

Figure 3: The elevation differences between global DEMs and the DSM in Psarrou, Mykonos. ASTER: left, SRTM: middle, TanDEM-X IDEM: right. (DX,DY,DZ)=(0,0,0).

Table 2: Bias and corresponding RMSEs of the 3 global DEMs over the 3 sites with respect to the recent DEM and DSM. (DX,DY,DZ) as defined in this table.

Result	Ref. DEM	Study site	ASTER	SRTM	TanIDEM-X
(DX,DY)	Recent DEM	Psarrou, Mykonos	*(-8,47)*	*(-30,46)*	*(4,1)*
		Chora, Chios	*(-18,3)*	*(-21,43)*	*(15,-1)*
		Vathi, Samos	*(3,5)*	*(-34,48)*	*(7,1)*
	DSM	Psarrou, Mykonos	*(-12,50)*	*(-36,50)*	*(-6,5)*
		Chora, Chios	*(-41,18)*	*(-27,45)*	*(2,2)*
		Vathi, Samos	*(6,-2)*	*(-39,51)*	*(7,2)*
$RMSE_{(DX,DY)}$	Recent DEM	Psarrou, Mykonos	7.5	3.9	2.5
		Chora, Chios	8.9	4.5	2.4
		Vathi, Samos	*8.3*	*5.2*	*1.7*
	DSM	Psarrou, Mykonos	7.7	4.0	2.5
		Chora, Chios	7.3	4.6	3.0
		Vathi, Samos	8.8	5.7	3.2
(DZ)	Recent DEM	Psarrou, Mykonos	(-4.6)	(0.1)	(-0.9)
		Chora, Chios	(-3.4)	(1.7)	(1.2)
		Vathi, Samos	(-5.7)	(0.5)	(0.0)
	DSM	Psarrou, Mykonos	(-4.9)	(0.1)	(-0.9)
		Chora, Chios	(-4.4)	(1.1)	(0.7)
		Vathi, Samos	(-4.7)	(-0.1)	(-0.7)
$RMSE_{(DX,DY,DZ)}$	Recent DEM	Psarrou, Mykonos	5.9	3.9	2.3
		Chora, Chios	8.2	4.2	2.0
		Vathi, Samos	6.0	5.2	1.7
	DSM	Psarrou, Mykonos	5.9	4.0	2.3
		Chora, Chios	5.8	4.5	2.9
		Vathi, Samos	7.4	5.7	3.1

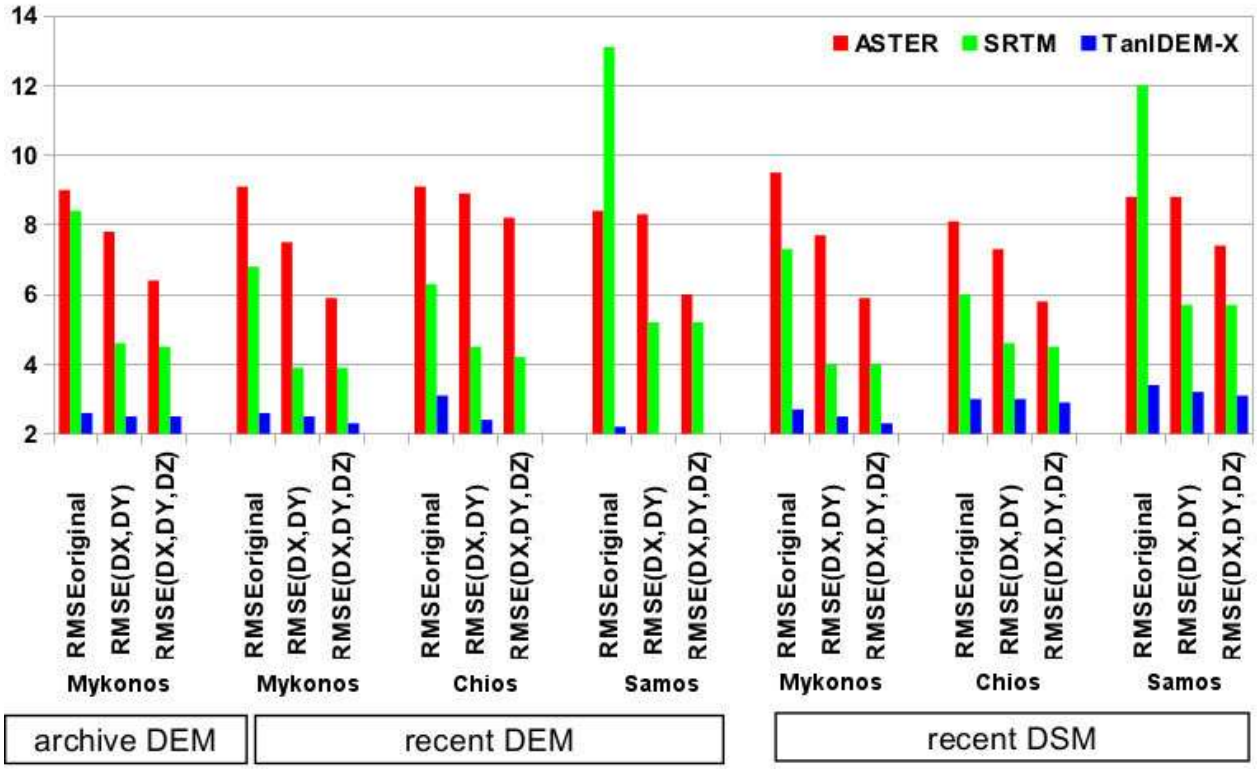

Figure 4: RMSE with no bias, RMSE with bias (DX,DY), and RMSE with bias (DX,DY,DZ) of the 3 global DEMs over the 3 sites with respect to the recent DEM and DSM.

Table 3: Bias and corresponding RMSEs of the 3 global DEMs over the 3 sites with respect to the recent DEM and DSM. (DX,DY,DZ) as defined in this table.

Result	Ref. DEM	Study site	TanIDEM-X
(DX,DY,DZ) Not weighted	Recent DEM	Psarrou, Mykonos	*(4,1,-0.9)*
		Chora, Chios	*(15,-1,1.2)*
		Vathi, Samos	*(7,1,0.0)*
$RMSE_{(DX,DY,DZ)}$ Not weighted	Recent DEM	Psarrou, Mykonos	2.3
		Chora, Chios	2.0
		Vathi, Samos	1.7
(DX_w,DY_w,DZ_w) HEM weighted	Recent DEM	Psarrou, Mykonos	(7, 1, 0.1)
		Chora, Chios	(9, -6, -0.5)
		Vathi, Samos	*(10, 8, 0.2)*
Criterion: $RMSE_{(DXw,DYw,DZw)}$ HEM weighted	Recent DEM	Psarrou, Mykonos	1.2
		Chora, Chios	1.0
		Vathi, Samos	0.5
$RMSE_{(DXw,DYw,DZw)}$ Not weighted	Recent DEM	Psarrou, Mykonos	2.5
		Chora, Chios	2.2
		Vathi, Samos	2.8

Finally the horizontal bias (DX, DY) and the vertical bias (DZ) between the TanDEM-X IDEM and the recent DEM were computed, taking into account the HEM metadata which accompanies TanDEM-X IDEM (equations 3, 4). Table 3 shows both the original (not weighted) bias (DX, DY, DZ) and the HEM weighted bias (DX_w, DY_w, DZ_w), as well as the corresponding RMSEs. It also

shows the criterion (equation 4) used for the computation of the weighted bias. It is evident that the inclusion of HEM affects not trivially the bias. And while the criterion is naturally less than the original (not weighted) RMSE, the RMSE of the new bias (DX_w, DY_w, DZ_w) is larger than the original RMSE and in the site of Vathi much larger (relatively). However, the new bias (DX_w, DY_w, DZ_w) is more realistic as it takes into account the known height errors of the TanDEM-X IDEM provided by HEM.

Tables 2 and 3 show that the horizontal and the vertical bias of TanDEM-X IDEM does not follow a trend, even at the same site but with different local DEM, and it looks random in nature. Furthermore, while the RMSE gets smaller when the bias is applied, it is gets only little smaller (less than 0.5 m). In contrast the RMSE of ASTER and SRTM gets much smaller (Figure 4). In fact the reduction of the RMSE of TanDEM-X IDEM (less than 0.5 m) is negligible compared to the accuracy given by TanDEM-X operator (less than 10 m), and thus the TanDEM-X IDEM has practically no bias.

CONCLUSIONS

In this paper, our previous research related to TanDEM-X IDEM and existing global DEMs over the Aegean islands was further extended in order to include more accurate elevation data and exploit the metadata of TanDEM-X IDEM. This paper verifies the results of the previous research: TanDEM-X is a more detailed and accurate global DEM compared to existing ones. Furthermore it has practically no bias with respect to local data which makes it easier to use and enhances its global applicability. Last but not least the Height Error Map (HEM) metadata of TanDEM-X IDEM in general leads to more realistic computations of the bias and possibly other properties, even though in the case of TanDEM-X IDEM the bias is negligible.

For further research we propose a more thorough study of coastline areas as TanDEM-X IDEM includes elevations in the sea area which have not been studied so far. Results computed in the present study imply that the quality of this new global DEM may be comparable to the one computed by satellite optical images. Further study of the TanDEM-X DEM from this point of view, would be an interesting topic for future research.

ACKNOWLEDGEMENTS

This research has been made for the research project “State-of-the-art mapping technologies for Public Work Studies and Environmental Impact Assessment Studies” (SUM). For the Greek side SUM project is co-funded by the EU (European Regional Development Fund/ERDF) and the General Secretariat for Research and Technology (GSRT) under the framework of the Operational Programme "Competitiveness and Entrepreneurship", "Greece-Israel Bilateral R&T Cooperation 2013-2015". The TanDEM-X IDEM data is provided by the German Space Agency (scientific proposal: IDEM-METH0140). The recent DEM and DSM data was created by the national mapping agency OKXE. The authors are grateful for the provision of the funding and the data.

REFERENCES

1 Bräutigam B, Martone M, Rizzoli P, Gonzalez C, Wecklich C, Borla Tridon D, Bachmann, M., Schulze D & Zink M, 2015. Quality assessment for the first part of the TANDEM-X global Digital Elevation Model. ISPRS - International Archives of the Photogrammetry, Remote Sensing and Spatial Information Sciences, XL-7/W3: 1137-1143, doi:10.5194/isprsarchives-XL-7-W3-1137-2015.

2 Moreira A, Krieger G, Hajnsek I, Hounam D, Werner M, Riegger S & Settelmeyer E, 2004. TanDEM-X: a TerraSAR-X add-on satellite for single-pass SAR interferometry. In Geoscience and Remote Sensing Symposium, 2004. IGARSS'04. Proceedings. 2004 IEEE International (Vol. 2, pp. 1000-1003). IEEE.

3 Krieger G, Moreira A, Fiedler H, Hajnsek I, Werner M, Younis M & Zink M, 2007. TanDEM-X: A satellite formation for high-resolution SAR interferometry. IEEE Transactions on Geoscience and Remote Sensing, 45(11): 3317-3341.

4 German Aerospace Center, 2013. TanDEM-X, Ground segment: DEM products specification document. Doc TD-GS-PS-0021, Issue 3.0, 43 p.

5 Vassilaki D I & Stamos A A, 2015. The 0.4 arc-sec TanDEM-X Intermediate DEM with respect to the SRTM and ASTER global DEMs. ISPRS - International Archives of the Photogrammetry, Remote Sensing and Spatial Information Sciences, XL-3/W2: 253-259, doi:10.5194/isprsarchives-XL-3-W2-253-2015.

6 Baade J & Schmullius C, 2015. Catchment properties in the Kruger National Park derived from the new TanDEM-X Intermediate Digital Elevation Model (IDEM). ISPRS - International Archives of the Photogrammetry, Remote Sensing and Spatial Information Sciences, XL-7/W3: 293-300, doi:10.5194/isprsarchives-XL-7-W3-293-2015.

7 Vassilaki D I & Stamos A A, 2014. Global DEMs' accuracy improvement with respect to local DEM data. 34th EARSeL Symposium Proceedings, 2.49–2.53.